Imaging Specific Protein Labels on Eukaryotic Cells in Liquid with Scanning Transmission Electron Microscopy

Diana B. Peckys,[1] Madeline J. Dukes,[2] Elisabeth A. Ring,[1] David W. Piston,[1] and Niels de Jonge[1] *

[1] Molecular Physiology and Biophysics, Vanderbilt University Medical Center, 2215 Garland Ave, Nashville, TN 37232-0615

[2] Department of Chemistry, Vanderbilt University, Nashville, TN 37235; present address: Protochips, Inc., Raleigh, NC 27606

* niels.de.jonge@vanderbilt.edu

Introduction

Understanding the structure and dynamics of the protein complexes that underlie cellular function is a central scientific challenge [1]. Biochemical techniques used to identify such complexes would be enhanced by the imaging of specific molecular positions in the context of intact cells, with protein-scale resolution (on the order of a few nanometers). Currently, though, nanometer resolution can only be achieved at the cost of less-direct imaging of the unperturbed cell. Cellular ultrastructure is traditionally studied by transmission electron microscopy (TEM), which yields nanometer resolution on embedded and stained sections, or cryo sections [2–4]. These cellular samples are neither intact nor in their native liquid state. Light microscopy is used to image protein distributions in fluorescently labeled cells in liquid to investigate cellular function [5], but even recent improvements in resolution by nanoscopy techniques [6, 7] are still insufficient to resolve the individual constituents of protein complexes. Thus, development of techniques capable of high-resolution imaging in native cellular states would contribute significantly to our understanding of cellular function at the molecular level. The development of liquid compartments that include electron-transparent silicon nitride membrane windows [8] has led to the introduction of a novel concept to achieve nanometer resolution on tagged proteins in cells [9].

Eukaryotic cells in liquid are placed in a microfluidic chamber, with a thickness of up to 10 µm, contained between two ultra-thin electron-transparent windows, as in Figure 1. The specimen is then imaged with the scanning transmission electron microscope (STEM). Due to the atomic number (Z) contrast of the STEM, nanoparticles of a high-Z material, such as gold, can be detected within the background signal produced by a low-Z liquid, such as water. Just as proteins tagged with fluorescent labels can be used to study protein distributions in cells with fluorescence microscopy, nanoparticles that are specifically attached to proteins [10] can be used to study protein distributions in whole cells in liquid, but with a much higher resolution. Liquid STEM can also be used in combination with bimodal probes that are visible with both fluorescence and electron microscopy, such as dye-conjugated gold nanoparticles or semi-conductor nanocrystals known as quantum dots (QDs) [11, 12]. An additional advantage of electron microscopy imaging of whole cells in liquid is the compatibility with sample preparation techniques used for light microscopy, that is, the absence of sectioning, freezing, and staining.

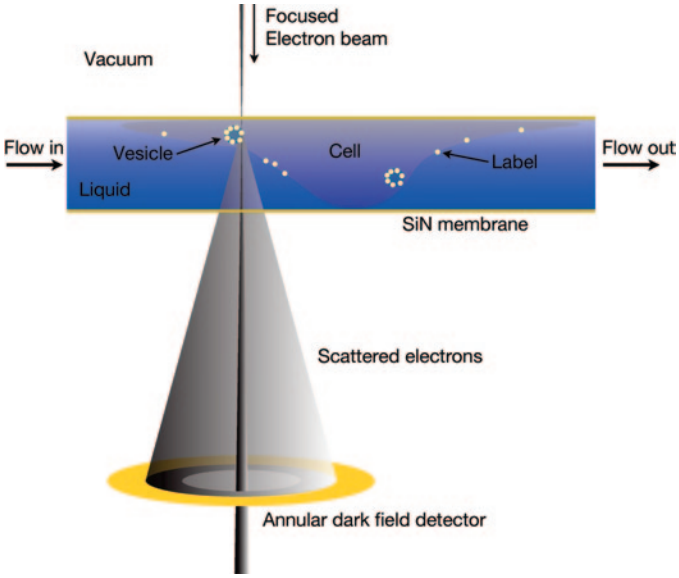

Figure 1: The principle of liquid scanning transmission electron microscopy (STEM). Cells kept in liquid are enclosed between two electron-transparent silicon nitride windows. Scanning a focused electron beam over the sample leads to the detection of elastically scattered electrons with an annular dark field detector. Labels of high atomic number materials can thus be distinguished. From [9].

Instrumentation

The main component of the liquid STEM system is a microfluidic chamber comprised of two silicon microchips, each supporting a 50 nm thick silicon nitride (SiN) window (Protochips, Inc., NC) [13, 14]. Figure 2A shows a scanning electron microscopy (SEM) image of the backside of a microchip. The dimensions of the microchip were 2.00 × 2.60 × 0.30 mm, and those of the SiN window were 50 × 200 µm. Two microchips were placed in the tip of a specimen holder for liquid flow (Protochips Inc., NC). The sides of the microchips were manufactured with a precision of ±10 µm with respect to the SiN window position to allow precise alignment of the windows when the two microchips were stacked. Precise alignment of the windows in the microfluidic chamber was needed for the electron beam to be transmitted through both windows, and this was achieved via the use of precision-made alignment poles in the slot of the tip (see Figure 2B). One of the microchips contained a spacer [14], typically 6 µm thick,

ROLERA™ thunder

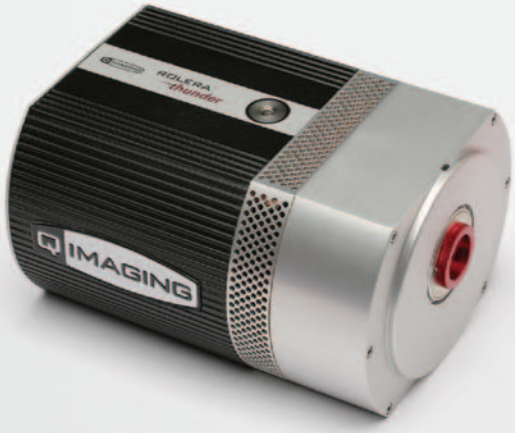

Introducing Rolera™ Thunder

The New EMCCD Camera from QImaging®

The latest addition to a new generation of high-sensitivity, low-light EMCCD cameras, Thunder is aggressively priced and loaded with unprecedented imaging capability.

Put Thunder in your research

Capture images that elucidate results

QIMAGING®

DIGITAL IMAGING MADE EASY

www.make-imaging-fun.com

info@qimaging.com

Learn more at WWW.QIMAGING.COM

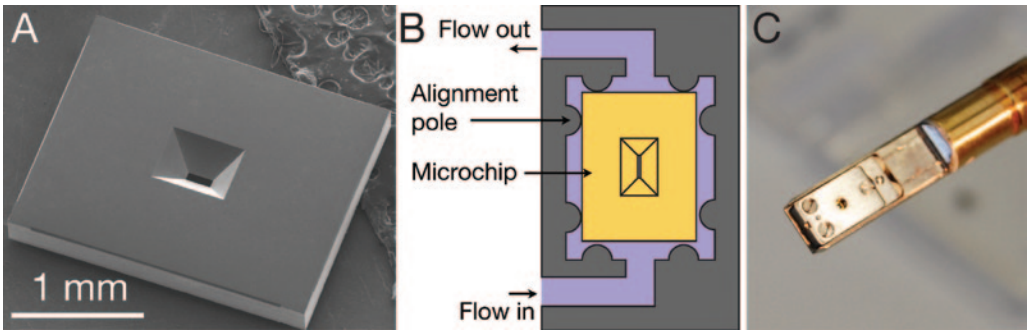

Figure 2: The microfluidic chamber for liquid STEM. (A) Scanning electron microscopy image showing the backside of a microchip with the silicon nitride window in the middle. (B) Schematic of the top view of the slot in the tip of the specimen holder in which the microchips are placed. The microchips are aligned at their sides via alignment poles. The liquid flow path runs through the chips. In addition, a second flow path, serving as a bypass channel, runs along the sides of the microchips. (C) The closed tip of the specimen holder, enclosing two microchips. The light shining through the windows indicates that both microchips are aligned. (This is not visible in the figure.)

to allow liquid to flow between the microchips and to provide a specimen chamber with sufficient height to contain thin eukaryotic cells; for example, COS7 fibroblast cells. In addition, the spacer defined a flow channel between two microchips over their long side. Figure 2C shows the closed tip of the specimen holder with the microfluidic chamber loaded in the interior. Light shining through the window indicated that alignment was achieved.

The liquid-flow specimen holder sealed the microfluidic chamber from the vacuum of the electron microscope via the use of O-rings. Plastic tubing connected the liquid specimen region to a syringe pump (Harvard Scientific, MA), which was outside of the electron microscope. Liquid was pumped from the syringe, through the microfluidic chamber in the tip of the holder, and back out of the microscope again. A photograph of the system is shown in Figure 3. The liquid STEM system consists of only three elements (the microfluidic chamber, the specimen holder, and the pump), transforming a standard STEM into a system for imaging specimens in liquid. Note that the system can be used for *in situ* electron microscopy of specimens in gaseous environments at atmospheric pressure [15]. The system also works for TEM imaging when a smaller spacer is used [16].

Results

Liquid STEM imaging of EGF-Au on COS7 cells. Liquid STEM images with 4 nm resolution were obtained on gold nanoparticle tagged proteins in whole eukaryotic cells in liquid [9]. COS7 fibroblast cells were labeled with 10 nm gold nanoparticles conjugated to epidermal growth factor (EGF). The cells were grown, labeled, and fixed with glutaradehyde directly on the microchips. The STEM was a 200 kV TEM/STEM (CM200, Philips/FEI, OR). Figure 4A shows the edge of a cell that was incubated for 5 minutes with EGF-Au. Gold labels are visible as green spots and the cellular material as light-blue matter over the dark-blue background. The localization of the labels at the cell edges after 5 minutes of label incubation is consistent with the physiological distribution of the EGF receptor, which is randomly dispersed over the cell surface [17]. The acquisition time for Figure 4A was 21 seconds for a 1024×1024 pixel image with a pixel-dwell time of $t = 20$ µs. The imaging speed can be increased simply by recording smaller images. The electron dose used for one image was $7 \cdot 10^4$ e$^-$/nm^2. The achieved spatial resolution was consistent with calculations and with results obtained on test samples containing gold nanoparticles [18].

To observe molecular rearrangements of the EGF receptors in the COS7 cells after ligand binding, a second batch of cells was incubated for 10 minutes with EGF-Au and then washed and incubated for an additional 15-minute period in buffer. Liquid STEM images of these cells are shown in Figure 4B. Circular clusters of labels are visible, consistent with the clustering of the EGF receptor in internalized endosomes after receptor activation [17].

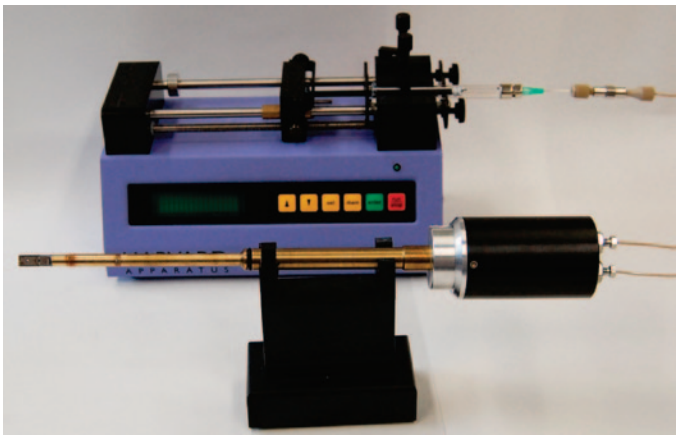

Figure 3: Photograph of the liquid STEM system including the specimen holder and a microfluidic syringe pump. Plastic tubing connects the liquid in the syringe with the microfluidic chamber at the tip of the specimen holder, which is placed in the vacuum chamber of the electron microscope.

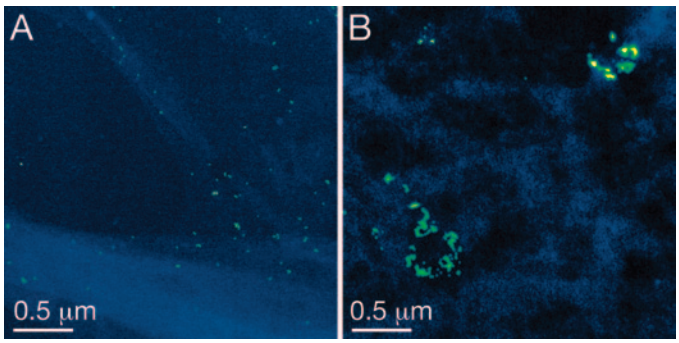

Figure 4: Liquid STEM images of gold-labeled epidermal growth factor (EGF) receptors on COS7 fibroblast cells. (A) Image of the edge of a fixed COS7 cell after 5 minutes of incubation with EGF-Au. The gold labels are visible as bright green spots on the blue background. The background shows some detail of the edge of the cell. (B) Image of a COS7 cell incubated with EGF-Au for 10 minutes and then incubated in buffer for an additional 15 minutes. The signal intensity was color-coded to increase the visibility of the labels. Images modified from [9].

Correlative fluorescence microscopy and liquid STEM of QD-labeled cells. COS7 fibroblast cells were grown on microchips, and the cells were incubated for five minutes with EGF conjugated to QD (EGF-QD) and then fixed with glutaraldehyde [12]. The cells were imaged on the microchip first by light microscopy, with the microchip placed upside-down (Figure 5) in a cell culture dish with phosphate-buffered saline. Figure 6A shows a fluorescence microscopy image of a window section partly covered with adhering cells. The QD labels light up as bright spots on cells against the dark background of cell-free regions. The cellular regions also contain faint fluorescence from the glutaraldehyde fixative. The microchip with cells was assembled into a microfluidic chamber along with a chip containing a spacer layer for liquid STEM imaging. Figure 6B shows a STEM image recorded at the edge of the same cell shown in Figure 6A. The lower two-thirds of the image contain bright spots of similar sizes, which we associate with the presence of QDs. The separation line between regions with and without QDs is interpreted as cell edge. Some debris left over from the microchip fabrication process is visible as well.

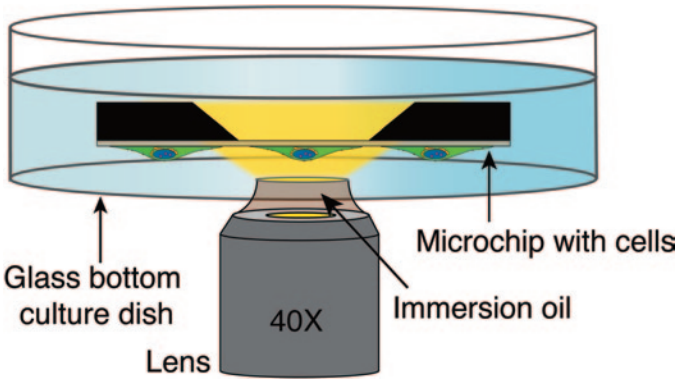

Figure 5: For imaging with light microscopy, prior to liquid STEM imaging, one of the microchips with the attached cells was placed upside down in a glass bottom culture dish and imaged using an oil-immersion lens. From [12].

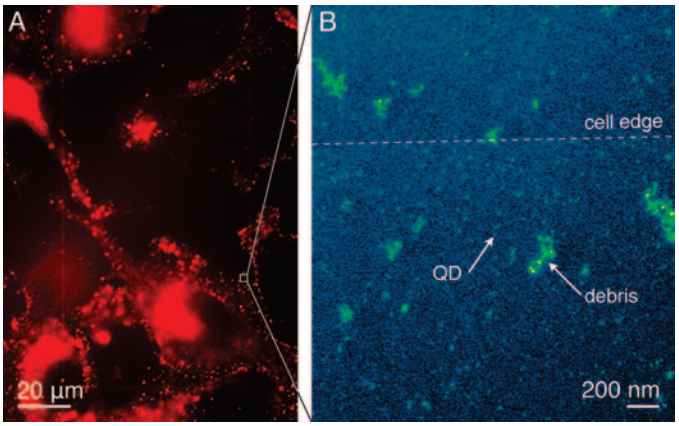

Figure 6: Correlative light microscopy and liquid STEM of intact fixed eukaryotic cells in saline water. (A) Red fluorescence signals from COS7 cells with QD-labeled EGF receptors. Some unspecific fluorescence from the fixative is also visible. The thin line at the left indicates the location of the silicon nitride window. (B) Liquid STEM image of the region indicated with a square in (A). Individual QDs along the edge of the cell can be discerned as green spots on a blue background. Some debris is also visible. The magnification was M = 48,000. The signal intensity was color-coded to increase the visibility of the labels. Figure modified from [12].

Localizing the same region in both light and electron microscopy images often requires dedicated procedures in correlative microscopy [19, 20]. For liquid STEM the localization was accomplished with a simple procedure. The positions of features in the fluorescence image were measured with respect to the frame of the SiN window, faintly visible in Figure 6A as a thin line. With the sample in the STEM, the position of one corner of the SiN window was located first. The stage position at this point was recorded and the scan rotation was aligned such that the scan direction of the electron beam ran parallel to the short side of the SiN window. During STEM imaging, the stage position of each image was recorded and correlated with the previously determined frame position of the SiN window. The position of Figure 6B corresponds to the square in Figure 6A. The position of the square in the fluorescent image is indeed at the edge of the cell.

Discussion

The spatial resolution achieved with liquid STEM of 4 nm and better on labeled proteins is on the order of the size of individual proteins. The high spatial resolution of liquid STEM obtained on sample volumes compatible with whole eukaryotic cells is not achievable with a liquid cell for TEM imaging [8] because the TEM contrast mechanism limits high-resolution imaging to a thickness of about 0.5 m. In the case of thin and weakly scattering samples, TEM yields a better resolution than STEM [21], but for the case of whole cells, STEM offers a particular advantage when imaging high-Z labels [22]. Imaging back-scattered electrons with a scanning electron microscope (SEM) from a specimen in liquid separated from the vacuum by a thin membrane [23, 24] provides a resolution of 8–20 nm on gold labels, but this is a surface technique that images only the top ~0.1 µm of the sample. The resolution of liquid STEM also surpasses alternative approaches, such as the imaging of cooled cells in water vapor using an environmental TEM [25, 26], environmental SEM with a STEM detector [27], or X-ray microscopy [28].

For fixed samples, liquid STEM presents a novel alternative to fluorescence microscopy. The resolution of liquid STEM is a factor of 50 higher than that of confocal microscopy. Current ultra-high-resolution optical methods include stimulated emission depletion (STED) [6, 29], photo-activated localization microscopy (PALM) [7], and stochastical optical reconstruction microscopy (STORM) [30]. Those techniques can obtain fluorescence images with a sub-diffraction spatial resolution of about 30 nm for practical imaging conditions of cells [31]. However, this length scale is still not sufficient to resolve the constituents of protein complexes, and the number of available orthogonal labels is limited.

The achieved spatial resolution of liquid STEM can be used to study protein distributions in cells and is sufficient to discriminate nanoparticles differing in size, shape, and electron density for multi-label experiments. A high-resolution liquid STEM image can thus provide information about the constituents of protein complexes with the context of

an intact fixed cell in liquid. Currently, liquid STEM is limited to surface proteins and proteins that internalize, but strategies for labeling intracellular proteins with high-Z labels [32, 33] may be used to label intracellular proteins in the future. Fluorescence microscopy may be used to monitor tagged proteins in living cells to determine the desired time point of the fixation, such that a specific state of the cell can subsequently be studied with liquid STEM; initial results show that liquid STEM of unfixed cells is also feasible [34]. By repeating the experiment, bringing the cells into different functional states, liquid STEM can be used to study cellular function at the level of protein complexes via a direct method. This should lead to a broad range of applications in biomedical research.

Conclusions

Liquid STEM is capable of imaging individual gold nanoparticles, labeling specific proteins in cells, as well as QDs labels, used for correlative fluorescence and electron microscopy. The sample preparation method for liquid STEM is similar to standard methods employed for light microscopy, with the difference that high-Z nanoparticle labels are needed to provide contrast in STEM. The images reveal the locations of protein labels with high resolution, while the biological structure is visible with less contrast, as is the case in fluorescence microscopy. Liquid STEM has a key advantage over state-of-the-art TEM: Cells are labeled live and then fixed. After this point, no further sample processing is required. Thus, artifacts often introduced by dehydration, post-staining, freezing, or sectioning are avoided. Liquid STEM combines some of the functionality of light microscopy with the resolution of electron microscopy.

Acknowledgments

We are grateful to J. Bentley, S. Head, G.J. Kremers, and T.E. McKnight for help with the experiments, and to Protochips Inc. for the liquid STEM system. A Portion of this research was conducted at the SHaRE User Facility, which is sponsored by the Division of Scientific User Facilities, Office of Basic Energy Sciences, U.S. Department of Energy. Research supported by Vanderbilt University Medical Center, NIH grant GM72048 (DWP), and NIH grant 1R43EB008589 (to S. Mick).

References

[1] A Sali, R Glaeser, T Earnest, and W Baumeister, *Nature* 422 (2003) 216–25.
[2] H Stahlberg and T Walz, *ACS Chem Biol* 3 (2008) 268–81.
[3] W Baumeister, *Prot Sci* 14 (2005) 257.
[4] V Lucic, F Foerster, and W Baumeister, *Annu Rev Biochem* 74 (2005) 833–65.
[5] J Lippincott-Schwartz, E Snapp, and A Kenworthy, *Nat Rev Mol Cell Biol* 2 (2001) 444–56.
[6] SW Hell, *Science* 316 (2007) 1153–58.
[7] E Betzig, GH Patterson, R Sougrat, OW Lindwasser, S Olenych, JS Bonifacino, MW Davidson, J Lippincott-Schwartz, and HF Hess, *Science* 313 (2006) 1642–45.
[8] MJ Williamson, RM Tromp, PM Vereecken, R Hull, and FM Ross, *Nat Mater* 2 (2003) 532–36.
[9] N de Jonge, DB Peckys, GJ Kremers, and DW Piston, *Proc Natl Acad Sci* 106 (2009) 2159–64.
[10] Y Xiao, F Patolsky, E Katz, JF Hainfeld, and I Willner, *Science* 299 (2003) 1877–81.
[11] G Gaietta, TJ Deerinck, SR Adams, J Bouwer, O Tour, DW Laird, GE Sosinsky, RY Tsien, and MH Ellisman, *Science* 296 (2002) 503–07.
[12] MJ Dukes, DB Peckys, and N de Jonge, *ACS Nano* 4 (2010) 4110–16.
[13] N de Jonge, DB Peckys, GM Veith, S Mick, SJ Pennycook, and CS Joy, *Microsc Microanal* 13 (suppl 2) (2007) 242–43.
[14] EA Ring and N de Jonge, *Microsc Microanal* 16 (2010) 622–29.
[15] N de Jonge, WC Bigelow, and GM Veith, *Nano Lett* 10 (2010) 1028–31.
[16] KL Klein, IM Anderson, and N de Jonge, *J Microscopy* 242 (2011) 117–23.
[17] DS Lidke, P Nagy, R Heintzmann, DJ Arndt-Jovin, JN Post, HE Grecco, EA Jares-Erijman, and TM Jovin, *Nat Biotechnol* 22 (2004) 198–203.
[18] N de Jonge, N Poirier-Demers, H Demers, DB Peckys, and D Drouin, *Ultramicroscopy* 110 (2010) 1114–19.
[19] DR Keene, SF Tufa, GP Lunstrum, P Holden, and WA Horton, *Microsc Microanal* 14 (2008) 342–48.
[20] BNG Giepmans, TJ Deerinck, BL Smarr, YZ Jones, and MH Ellisman, *Nat Meth* 2 (2005) 744–49.
[21] P Rez, *Ultramicroscopy* 96 (2003) 117–24.
[22] DB Peckys, GM Veith, DC Joy, and N de Jonge, *PLoS One* 4 (2009) e8214.
[23] S Thiberge, A Nechushtan, D Sprinzak, O Gileadi, V Behar, O Zik, Y Chowers, S Michaeli, J Schlessinger, and E Moses, *Proc Natl Acad Sci* 101 (2004) 3346.
[24] H Nishiyama, M Sugo, T Ogura, Y Maruyama, M Koizumi, K Mio, S Kitamura, and C Sato, *J Struct Biol* 169 (2010) 438–40.
[25] TL Daulton, BJ Little, K Lowe, and J Jones-Meehan, *Microsc Microanal* 7 (2001) 470–85.
[26] PL Gai, *Microsc Microanal* 8 (2002) 21–28.
[27] A Bogner, G Thollet, D Basset, PH Jouneau, and C Gauthier, *Ultramicroscopy* 104 (2005) 290–301.
[28] MA Legros, G McDermott, and CA Larabell, *Curr Opin Struct Biol* 15 (2005) 593–600.
[29] KI Willig, SO Rizzoli, V Westphal, R Jahn, and SW Hell, *Nature* 440 (2006) 935–39.
[30] M Bates, B Huang, GT Dempsey, and X Zhuang, *Science* 317 (2007) 1749–53.
[31] J Lippincott-Schwartz and S Manley, *Nat Meth* 6 (2009) 21–23.
[32] LY Chou, K Ming, and WC Chan, *Chem Soc Rev* 40 (2011) 233–45.
[33] X Shu, V Lev-Ram, TJ Deerinck, Y Qi, EB Ramko, MW Davidson, Y Jin, MH Ellisman, and RY Tsien, *PLoS Biol* 9 (2011) e1001041.
[34] DB Peckys, P Mazur, KL Gould, and N de Jonge, *Biophys J* 100 (2011) 2522–29.

MT

AURIGA®

Information Beyond Resolution

Unique Imaging | Precise Processing | Advanced Analytics | Future Assured

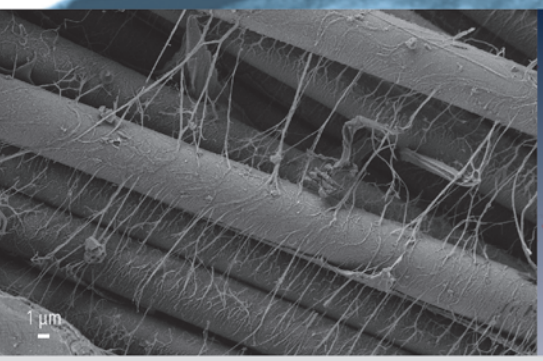

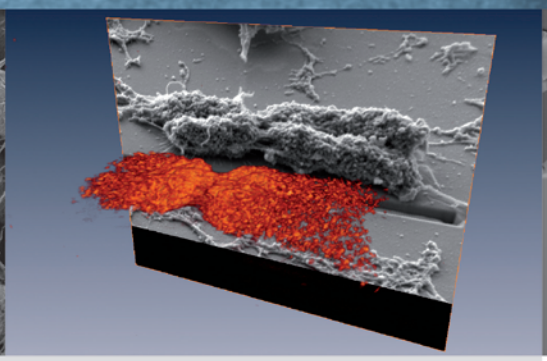

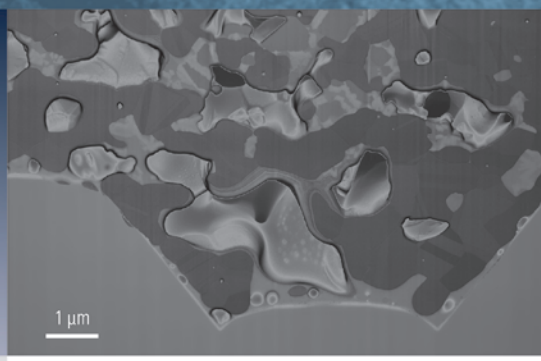

Carl Zeiss NTS, LLC
One Corporation Way
Peabody, MA 01960, USA
Tel. +1 978 / 826 1500
Fax +1 978 / 532 5696
info-usa@nts.zeiss.com
www.zeiss.com/nts

ZEISS

We make it visible.